

## A Unified View of Surface-Enhanced Raman Scattering

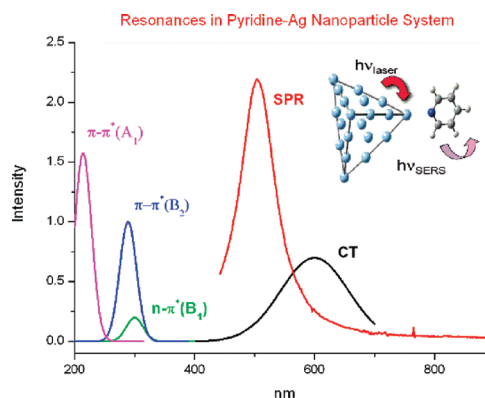
JOHN R. LOMBARDI\* AND RONALD L. BIRKE

Department of Chemistry, The City College of New York, New York, New York 10031

RECEIVED ON NOVEMBER 5, 2008

### CON SPECTUS

In the late 1970s, signal intensity in Raman spectroscopy was found to be enormously enhanced, by a factor of  $10^6$  and more recently by as much as  $10^{14}$ , when an analyte was placed in the vicinity of a metal nanoparticle (particularly Ag). The underlying source of this huge increase in signal in surface-enhanced Raman scattering (SERS) spectroscopy has since been characterized by considerable controversy. Three possible contributions to the enhancement factor have been identified: (i) the surface plasmon resonance in the metal nanoparticle, (ii) a charge-transfer resonance involving transfer of electrons between the molecule and the conduction band of the metal, and (iii) resonances within the molecule itself. These three components are often treated as independently contributing to the overall effect, with the implication that by properly choosing the experimental parameters, one or more can be ignored. Although varying experimental conditions can influence the relative degree to which each resonance influences the total enhancement, higher enhancements can often be obtained by combining two or more resonances. Each resonance has a somewhat different effect on the appearance of the resulting Raman spectrum, and it is necessary to invoke one or more of these resonances to completely describe a particular experiment. However, it is impossible to completely describe all observations of the SERS phenomenon without consideration of all three of these contributions. Furthermore, the relative enhancements of individual spectral lines, and therefore the appearance of the spectrum, depend crucially on the exact extent to which each resonance makes a contribution.



In this Account, by examining breakdowns in the Born–Oppenheimer approximation, we have used Herzberg–Teller coupling to derive a single expression for SERS, which includes contributions from all three resonances. Moreover, we show that these three types of resonances are intimately linked by Herzberg–Teller vibronic coupling terms and cannot be considered separately.

We also examine the differences between SERS and normal Raman spectra. Because of the various resonant contributions, SERS spectra vary with excitation wavelength considerably more than normal Raman spectra. The relative contributions of totally symmetric and non-totally symmetric lines are also quite different; these differences are due to several effects. The orientation of the molecule with respect to the surface and the inclusion of the metal Fermi level in the list of contributors to the accessible states of the molecule–metal system have a strong influence on the observed changes in the Raman spectrum.

### Introduction

Since its inception in the late 1970s, surface-enhanced Raman scattering (SERS)<sup>1–5</sup> has proven to be a resilient and intriguing subject, engendering thousands of articles and along with these considerable controversy as well. The discovery of an enormous enhancement in the Raman intensity

when a molecule is in the vicinity of a metal (usually Ag) nanoparticle, coupled with the suppression of fluorescence, suggests the possibility that SERS could provide an invaluable tool as a reliable, high-resolution detection technique for extremely minute quantities of target molecules. Indeed recent technical advances have shown the

way to detection on the single-molecule (SM) level,<sup>6–12</sup> suggesting enhancement factors as large as  $10^{14}$ . These studies indicate that special sites, sometimes referred to as “hot spots” are responsible for a large portion of the observed enhancement. In fact this possibility was suggested some time ago by poisoning certain sites on a silver surface with under-potential deposition of Pb and Tl.<sup>13,14</sup> A mere surface coverage of 3% was sufficient to completely quench the SERS signal. Hildebrandt and Stockburger<sup>15</sup> showed that for rhodamine 6G adsorbed on silver colloid, anion activated specific sites are formed at extremely low surface coverage and that these sites are responsible for a large portion of the enhancement. A careful surface-dependent study by Zeman et al.<sup>16</sup> indicated that at coverages as low as 0.07 of a monolayer, the enhancement factor peaks, and it rapidly becomes lessened at higher coverage.

For a long time, there was considerable debate as to the exact source of the enhancement. However, most investigators in the field now agree that there are at least three possible sources for the enhancement.<sup>17–20</sup> The one most often cited is the existence of surface plasmon resonances (SPR) due to collective excitation of electrons in the conduction band of the metal nanoparticle. Numerous experiments and theoretical approaches have been invoked to demonstrate the importance of SPR's and to find ways to optimize and control the influence of these resonances. The second important contribution was first observed electrochemically, in which Raman resonances could be obtained by varying the applied potential. The observed wavelength dependence of these resonances showed that charge transfer (CT) between the molecule and the metal conduction band was responsible for this effect.<sup>21–26</sup> This charge transfer can occur in either direction depending on the relative energies of the metal Fermi level and the HOMO and LUMO levels of the adsorbed molecule, and we have shown experimentally that the CT does take place in both directions, that is, metal cluster-to-molecule or molecule-to-metal cluster, depending on the nature of the molecule.<sup>23</sup> Molecules with low-lying unfilled  $\pi$  orbitals (such as pyridine) experienced metal-to-molecule transfer, while those without low-lying unfilled orbitals (such as  $\text{NH}_3$  or piperidine) tended to transfer electrons to the metal. The third possible contribution to the overall effect was shown to be due to resonances within the adsorbed molecule itself. This effect is especially important in providing a boost to the Raman intensity enabling the single-molecule effect to be more easily observable. As we will show below, each of these resonances have a somewhat different effect on the appearance of the resulting Raman spectrum, and it is found necessary to

invoke one or more of these resonances in order to completely describe a particular experiment. However, it is impossible to completely describe *all* the observations of the SERS phenomenon by ignoring one of these contributions.

Most of the theories of the enhancement mechanism that have been proposed only treat one mechanism, namely, the SPR effect. Furthermore, even when a physical model of the SERS phenomenon invokes the coupling of two resonances (SPR and CT) to explain the enhancement magnitude such as the model of Otto and co-workers,<sup>27</sup> they are formulated in a way that does not provide a quantitative description of the spectroscopy. Thus, we felt as early as the mid 1980s that an adequate theory of SERS should predict the relative enhancement of bands of different symmetry in the SERS spectrum.<sup>17</sup> Such a model should account for all three types of resonance. Since these three effects appear to be quite disparate, it is understandable that theoretical models of SERS have not treated the resonances in a uniform way. In fact, they are often described in quite different terms, as though they were just coincidental contributors. One of the reasons for this is that the three effects make wildly varying degrees of contribution to the overall enhancement, depending on the nature of the nanoparticle, the nature of the molecule, and the exact location of the excitation laser wavelength. Each of the three resonances may occur in very different regions of the spectrum and may have different widths and oscillator strengths, so a complete analysis of the relative contributions requires a rather extensive range of excitations, often a difficult experimental undertaking. A typical Raman experiment, however, is often carried out only at a single (or at most just a few) excitation wavelength. Under these circumstances, it is impossible to unravel the magnitude of each contribution to the overall enhancement, and any statement as to the apparent source or sources of the effect measured at a single wavelength is risky.

We therefore have been motivated to search for a single, unified expression for the SERS intensity that incorporates all three effects and therefore identifies the source of each contribution, identifies the parameters that govern the amount of the contribution, and provides a systematic approach for an experimental determination of these contributions. It is the purpose of this Account to examine such an expression and discuss its implications for the systematic analysis of surface enhancement effects.

## A Unified Expression for SERS

In order to obtain an analytical expression for the Raman intensity in the proximity of one or more metal nanoparticles,

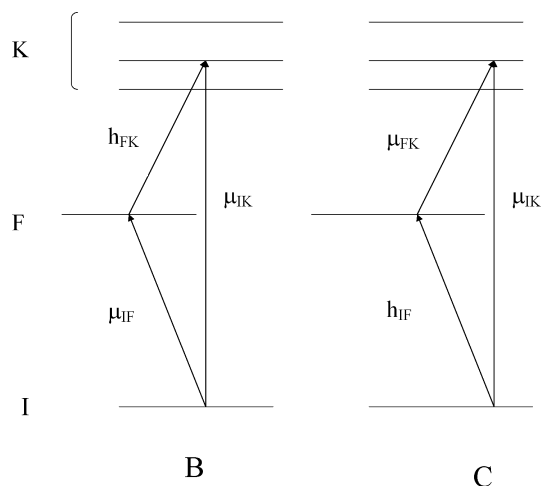


**FIGURE 1.** Energy level diagram of the metal–molecule system for the *B* and *C* polarizability terms showing electronic transition moments and Herzberg–Teller coupling parameter. *I* and *K* are molecular states, while *F* is a charge-transfer state.

we followed the procedure of Albrecht,<sup>28</sup> introducing Herzberg–Teller vibronic coupling into the expression for the polarizability. This is carried out to second order in perturbation theory by allowing for breakdowns in the Born–Oppenheimer approximation. We extended the calculation of Albrecht by considering the molecule–metal system to be coupled and including the filled and unfilled levels of the conduction band of the metal in the Herzberg–Teller expansion. Replacing the sum over metal states with an integral, we showed that the maximum enhancement occurs when transitions to or from the (unfilled or filled) metal levels is at the Fermi energy.<sup>17</sup> The resulting expression is analogous to that of Albrecht in that the polarizability ( $\alpha$ ) can be expressed as a sum of three terms:  $\alpha = A + B + C$ , where *A* is a sum of terms with only Franck–Condon integrals in the numerators. Far from a resonance, it vanishes, while near a resonance, one of the terms in the expression for *A* can become large. However, only totally symmetric Raman lines are allowed by this term. It is usually considered to be responsible for resonance Raman spectra. The sums *B* and *C* represent Herzberg–Teller contributions and stem from molecule-to-metal or metal-to-molecule charge-transfer transitions, respectively (see Figure 1). These transitions are said to “borrow” intensity from nearby allowed molecular transitions via the Herzberg–Teller coupling constant (*h*). These sums display allowed transitions both to totally symmetric and to non-totally symmetric vibrational modes and the resulting intensity can be enhanced by SPR or charge-transfer processes. Whenever SERS spectra display intensity in non-totally symmetric normal modes, the *B* or *C* sums or both *must* be involved. They may also contribute to the totally symmetric bands, as do the *A* expressions. In a

region of the SERS spectrum far from either a charge-transfer or molecule resonance, where only SPR resonances are important, the *A* term does not contribute. It can be shown that in this spectral region the *B* and *C* sums are entirely responsible for the SERS intensity. The analytic expressions for *B* and *C* involve infinite sums over all the states of the molecule–metal system, and as such are rather unwieldy. However, when the excitation wavelength is in the region of a charge-transfer or molecular resonance (in addition to the SPR), only one or a very few of these terms will dominate the sum. We may express one of these terms as<sup>18</sup>

$$R_{iFK}(\omega) = \frac{\mu_{KK}\mu_{FK}h_{iF}\langle j|Q_k|f\rangle}{((\varepsilon_1(\omega) + 2\varepsilon_0)^2 + \varepsilon_2^2)(\omega_{FK}^2 - \omega^2 + \gamma_{FK}^2)(\omega_{IK}^2 - \omega^2 + \gamma_{IK}^2)} \quad (1)$$

The surface-enhanced Raman intensity is proportional to the square of the polarizability and therefore, for a single dominant term, to  $|R_{iFK}(\omega)|^2$ . In this expression, *I*, *F*, and *K* refer to the ground state, a charge-transfer state, and an excited molecular state of the molecule–metal system, respectively.<sup>29</sup> Let us first examine the denominator, which involves the product of three terms, each of which depicts a different resonance contribution to SERS. The first  $(\varepsilon_1(\omega) + 2\varepsilon_0)^2 + \varepsilon_2^2$  is due to the plasmon resonance at  $\varepsilon_1(\omega) = -2\varepsilon_0$ , where  $\varepsilon_1$  and  $\varepsilon_2$  are the real and imaginary parts of the Ag dielectric constant and  $\varepsilon_0$  is the real part of the dielectric constant of the surrounding medium. We choose the expression for a single particle for illustrative purposes, recognizing that for non-spherical particles or particle aggregates with hot spots a more complex expression containing a similar dielectric resonance expression will be required. The second resonance, which may be potential (Fermi energy)-dependent and represents charge-transfer resonance  $(\omega_{FK}^2 - \omega^2) + \gamma_{FK}^2$  occurs at  $\omega = \omega_{FK}$ , and the third  $(\omega_{IK}^2 - \omega^2) + \gamma_{IK}^2$  represents a molecular resonance at  $\omega = \omega_{IK}$ . For electrochemical SERS, the expression for the second resonance in the *C* term predicts a positive slope for  $V_{MAX}$  (the applied voltage at resonance) against  $\omega$  for metal-to-molecule transfer, and the *B* term predicts the opposite (negative) slope for molecule-to-metal transfer ( $\hbar\omega = \hbar\omega_{F,K} = E_F(0) \pm eV_{MAX}$ ).<sup>23,30</sup> This is illustrated for several molecules in Figure 2, where we show the potential maximum ( $V_{MAX}$ ) as a function of excitation energy ( $\hbar\omega$ ). It can be seen that molecules such as piperidine and quinuclidine, without low-lying  $\pi^*$  orbitals to accept electrons, display a negative slope, while for pyridine, *p*-aminothiophenol (PATP), and 4-methyl pyridine, there is a positive slope. Note, in the third case, if the reso-

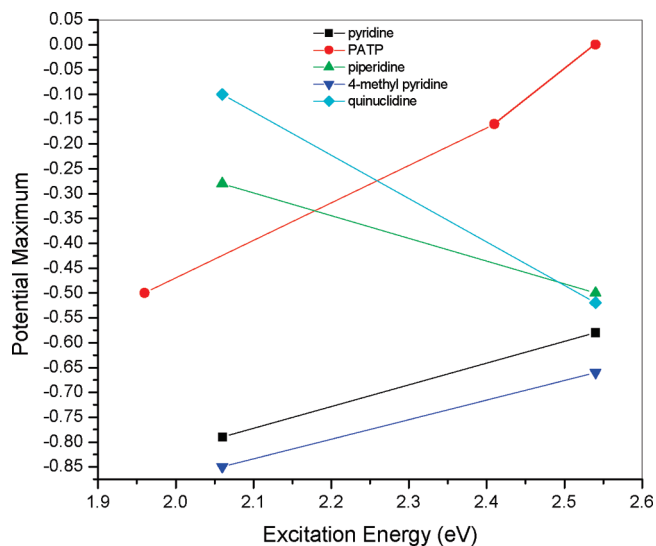


**FIGURE 2.** SERS potential of maximum intensity,  $V_{\text{MAX}}$ , vs excitation energy showing the direction of CT for various molecules. Molecules such as piperidine and quinuclidine display a negative slope (molecule  $\rightarrow$  metal), while for pyridine, *p*-aminothiophenol (PATP), and 4-methyl pyridine, there is a positive slope (metal  $\rightarrow$  molecule).

nance condition is fulfilled ( $\omega = \omega_{\text{IK}}$ ), we have SERS (surface-enhanced resonance Raman spectroscopy). This is the case for most of the single-molecule experiments, for which the molecular transition is also in resonance with the laser.

Even without electrochemical SERS studies, it is possible to predict whether a CT resonance will occur if good estimates of the Fermi level of the solid substrate and of the energy levels of the molecule at the surface are available. This can be illustrated for crystal violet cation,  $\text{CV}^+$ , where reduction potentials of crystal violet cation for one-electron oxidation and reduction establish approximate energy levels ( $\pm 0.1$  eV) of HOMO and LUMO levels of the molecule in solution, and the electrode potential gives the Fermi level of the metal relative to the molecular levels. Figure 3 shows the energy level diagram obtained from electrochemistry.<sup>31</sup> The electrochemical HOMO–LUMO gap of 1.9 eV is almost identical to the lowest optical singlet  $\pi-\pi^*$  transition. Thus, if the Fermi energy of the metal is around  $-4.1$  eV, light of 2 eV (633 nm) will simultaneously excite both a molecule-to-metal CT transition and the  $\pi-\pi^*$  molecular resonance, the latter with oscillator strength around 0.8.<sup>31</sup> In agreement with this conclusion, an electrochemical SERS study of  $\text{CV}^+$  on a Ag surface showed a  $V_{\text{MAX}}$  of  $-0.5$  V vs SCE reference electrode.<sup>32</sup>

In Figures 4 and 5, we illustrate the various resonances in a molecule–metal system for two commonly studied molecules, pyridine (Figure 4) and crystal violet cation (Figure 5). In Figure 4, there are three distinct regions. The pyridine absorption spectrum involves three transitions in the ultraviolet (two

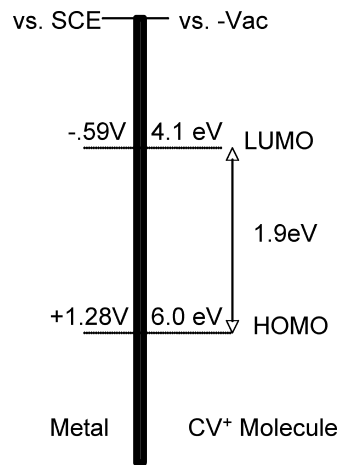


**FIGURE 3.** Energy level diagram showing levels in the  $\text{CV}^+$  molecule vs the vacuum level and the corresponding levels in a metal electrode vs SCE reference. The relationship between the two energy scales is that the hydrogen reduction potential vs SCE is  $-0.24$  V, which corresponds to a Fermi level of  $-4.5$  eV on an absolute scale.

#### Resonances in Pyridine–Ag Nanoparticle System

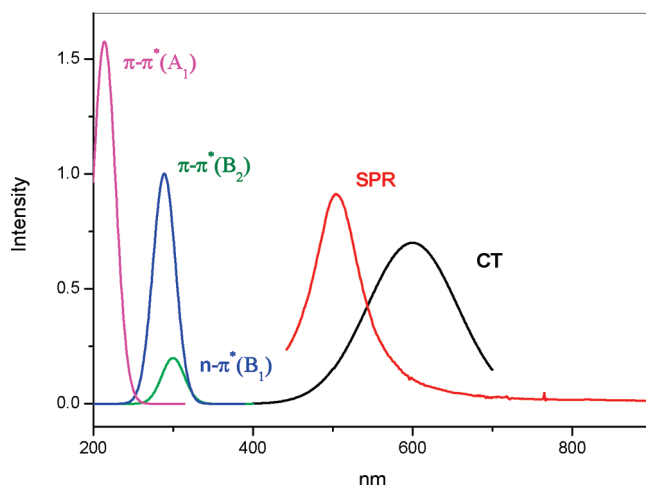


**FIGURE 4.** Observed resonances in the pyridine–Ag nanoparticle system. Data taken from refs 33 and 39 (SPR), ref 40 (molecular resonances), and refs 41 and 42 (charge-transfer).

$\pi-\pi^*$  and one  $n-\pi^*$  transitions). In the near-UV and visible are a surface plasmon resonance<sup>33</sup> and a molecule-to-metal charge-transfer resonance, which overlap between about 480 and 520 nm. It can be seen that by restricting the laser to wavelengths lower than around 480 nm, only the surface plasmon resonance will be excited, while as the wavelength is increased, a mixture of CT and SPR will contribute to the overall enhancement. While there are no molecular resonances excited in this region, it can be seen from eq 1 that intensity can be borrowed from them via Herzberg–Teller coupling and the amount of borrowing is proportional to the square of the transition moments (i.e., the oscillator strengths) of the molecular transition. Figure 5 shows the absorption



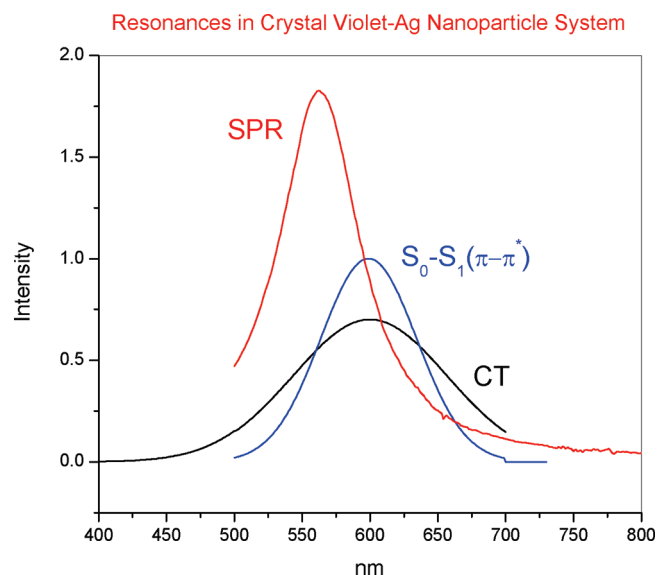


**FIGURE 5.** Observed resonances in the crystal violet cation–Ag nanoparticle system. Data taken from refs 33 and 39 (SPR), ref 43 (molecular resonance), and refs 44 and 45 (charge-transfer).

spectrum of the crystal violet–metal system, where all three resonances are in the visible region and overlap with the highest intensity around 575 nm, which is prognostic of single-molecule SERS. This explains why crystal violet is so popular in single-molecule SERS. Here the energy level diagram (Figure 3) shows that the LUMO of the molecule is too low for metal-to-molecule CT if the Fermi level of Ag is close to  $-4.1$  eV but molecule-to-metal transitions can be in resonance when the exciting light is around 600 nm.

The denominator of eq 1 predicts the possibility of one, two, or three resonances simultaneously, depending on the metallic and molecular parameters. The exact magnitude of the enhancement, the relative contribution of each of the three possible types of resonances involved, and the appearance of the Raman spectra (i.e., the relative intensities of the various bands) depend crucially on the particular choice of excitation wavelength, location of the nanoparticle Fermi energy, nanoparticle size and shape with respect to the wavelength, oscillator strength, and bandwidth of the resonance. This is illustrated clearly in Figures 4 and 5. It should also be pointed out that at any of the resonances, the enhancement factor is proportional to the inverse fourth power of the corresponding damping parameter,  $\gamma^{-4}$  (where  $\gamma$  is  $\varepsilon_2$ ,  $\gamma_{FK}$ , or  $\gamma_{IK}$ ). Thus the magnitude of the SERS enhancement may be extremely sensitive to the magnitude of these parameters.

We should also remember that in general the SERS intensity is proportional to the square of the polarizability ( $\alpha$ ), which itself is, most generally, a sum of terms such as eq 1. Under circumstances in which the relative signs of leading terms differ, interference can result, with a net lowering of the inten-

sity. Such interferences have been observed<sup>34</sup> in J-aggregate nanoparticle systems and explained by Kelley in terms of Fano-like resonances<sup>35</sup> using dipole–dipole (Förster) coupling between molecule and metal nanoparticle.<sup>36</sup> However, such interference effects can also be explained within the current framework of Herzberg–Teller coupling. This coupling mechanism is the major difference between the two approaches.

We now examine the numerator in eq 1, which provides the selection rules for SERS. All four terms must simultaneously be nonzero in order for a particular normal mode to be observed. *It is important to observe that all four terms in the numerator are linked to each other.* This fact has not always been appreciated in discussions of SERS enhancements. First note that the Herzberg–Teller effect contributes a product of the coupling parameter  $h_{IF} = \langle i | \partial V_{eN} / \partial Q_k | F \rangle$  with the vibrational integral  $\langle i | Q_k | f \rangle$ . The normal mode  $Q_k$  is the same in both expressions. The latter  $\langle i | Q_k | f \rangle$  displays the normal harmonic oscillator selection rules (i.e.,  $f = i \pm 1$ ), and only those normal modes for which this term is nonzero will be observed. Note that this term implies that overtones will not normally be observed and that non-totally symmetric vibrations may be allowed. However, an additional restriction on observed modes is provided by the Herzberg–Teller coupling term,  $h_{IF}$ , which must simultaneously be nonzero for the normal mode  $Q_k$  to be observed. This additional selection rule is crucial for understanding the details of SERS spectra. The other two terms in the numerator involve a product of the dipole transition moments  $\mu_{IK}^k \mu_{FK}^k$ , which are the allowed molecular transition I–K and the (metal–molecule) charge-transfer transition F–K. The charge-transfer or molecular transition moment will depend on the molecular orientation with respect to the metal and therefore depends on the geometry of the molecule–metal complex. Since the maximum electric field due to the plasmon resonance is normal to the metal surface, and the electric field interacts with the dipole moments through the inner product ( $\boldsymbol{\mu} \cdot \mathbf{E}$ ), we expect components of  $\mu_{FK}^{\rho}$  and  $\mu_{KI}^{\sigma}$  normal to the surface (i.e.,  $\rho, \sigma = Z$ ) to provide the major contribution to SERS. Weaker contributions from either  $\sigma$  or  $\rho = X, Y$  will also be expected. Note that the combination of transition moments, Herzberg–Teller coupling, and direction of the plasmon-induced electric field places restrictions on the nature of the spectrum and the symmetry of the normal modes expected to be observed. In the next section, we examine the consequences of these restrictions for observed SERS spectra.

It is important to understand how the product of terms in the numerator links the three resonances in the denominator. The charge-transfer transition moment ( $\mu_{FK}^{\rho}$ ) is coupled with

the component of the electric field due to the surface plasmon resonance perpendicular to the surface ( $\rho = Z$ ). This requires knowledge of the orientation of the molecule with respect to the surface.<sup>37</sup> It also shows that the surface plasmon and the charge transfer are intimately coupled to each other and are not separable. Furthermore, the charge-transfer resonance is linked to the molecular resonance by the molecular transition moment ( $\mu_{\text{K}}^{\sigma}$ ) since they both refer to the same excited-state K. Consequently, these two resonances cannot be considered to be separate. The Herzberg–Teller coupling constant ( $h_{\text{IF}} = \langle I | \partial V_{\text{eN}} / \partial Q_{\text{k}} | F \rangle$ ) provides the link between the charge-transfer process (F) and the observed Raman spectral lines governed by  $\langle j | Q_{\text{k}} | f \rangle$ . Thus the three resonances that contribute to SERS intensities *cannot be considered separately*, and any description of SERS must include this linkage in order to provide a complete and accurate depiction of the effect.

## SERS Selection Rules

We can now utilize the considerations in the previous section to express, in a rather simple fashion, the selection rules governing SERS intensities. These are derived from the requirement that the numerator in eq 1 not vanish. Since this involves the product of the three terms,  $\mu_{\text{K}}^{\sigma} \mu_{\text{FK}}^{\rho} h_{\text{IF}} = \langle I | \mu^{\sigma} | K \rangle \langle K | \mu^{\rho} | F \rangle \langle F | \partial V_{\text{eN}} / \partial Q_{\text{k}} | I \rangle$ , rather strict selection rules are expected (see Figure 1). We wish to examine the irreducible representation to which an allowed Raman transition belongs  $\Gamma(Q_{\text{k}})$  ( $= \Gamma(\partial/\partial Q_{\text{k}})$ ). Since the molecule–metal states I, F, and K all appear twice in the numerator expression, together they provide only totally symmetric contributions to the selection rules. We then need only consider the irreducible representations for the operators  $\Gamma(\partial/\partial Q_{\text{k}})$ ,  $\Gamma(\mu_{\text{CT}}^{\perp})$ , and  $\Gamma(\mu_{\text{K}}^{\sigma})$ . Here  $\Gamma(\mu_{\text{CT}}^{\perp})$  is the component of the charge-transfer moment normal to the metal surface. In the molecule-fixed frame of reference, it depends on the molecular orientation with respect to the surface. Consideration of  $\Gamma(\mu_{\text{K}}^{\sigma})$  indicates that if the ground-state is totally symmetric, then  $\Gamma(\mu_{\text{K}}^{\sigma}) = \Gamma_{\text{K}}$ , the irreducible representation to which the excited molecular state K belongs. Then the Herzberg–Teller selection rules may be simply expressed as

$$\Gamma(Q_{\text{k}}) = \sum_{\text{K}} \Gamma(\mu_{\text{CT}}^{\perp}) \times \Gamma_{\text{K}} \quad (2)$$

Here the sum over K runs over all the excited molecular states to which a transition is allowed. For SERRS, this sum reduces to a single term choosing K as the excited-state involved in the molecular resonance.

It should also be noted that what is meant by an “allowed” optical transition is not as definite as implied by strict application of the selection rules. Even transitions that are optically forbidden are often made at least somewhat allowed by interactions with the surroundings, intervention of external fields, or other previously neglected higher order terms in the Hamiltonian. Thus we must qualify our above discussion by recognizing that the SERS intensities will be proportional to the square of  $\mu_{\text{K}}^{\rho}$ , which is sometimes referred to as the oscillator strength  $f_{\text{Kl}} \propto (\mu_{\text{K}}^{\rho})^2$ . We might then expect that the relative intensities of the SERS bands of a given symmetry will be proportional to the relative oscillator strengths of the observed optical transitions. For example, by consideration of the optical spectrum of pyridine–Ag (Figure 4), we see that the UV transition oscillator strengths are in the order  $A_1 > B_2 > B_1$ , so that we then predict the SERS intensities of the normal modes to be in the order  $a_1 > b_2 > b_1$ , which is exactly as observed. We have shown this to be true for the SERS spectra of all molecules examined with sufficient symmetry and measured oscillator strengths.<sup>18</sup> However, there are also other contributing factors such as the square of the Herzberg–Teller coupling constant ( $h_{\text{IF}}^2$ ), which must be taken into account in predicting relative SERS intensities.

## What Is the Difference between SERS and Normal Raman Spectroscopy?

If we quickly examine the general expressions for SERS (ref 18, eq 10) and the corresponding expression for normal Raman spectroscopy (ref 28, eq 11), they at first appear to be quite similar. They both involve large sums of terms similar to eq 1 above. However, more careful examination reveals that one difference is the inclusion of charge-transfer (F) states between the molecule and metal. This comes about because we consider the molecule–metal system together. Note that for metals, the Fermi level lies above the highest occupied molecular orbital (HOMO) of most molecules (for silver  $E_{\text{F}} = -4.3$  eV and for pyridine the IP is  $-9.26$  eV), and often lower than many, if not all, of the unoccupied orbitals (UMO). Thus for every molecular transition (HOMO  $\rightarrow$  UMO), there is a corresponding charge-transfer transition between the molecule and the metal ( $E_{\text{F}} \rightarrow$  UMO or HOMO  $\rightarrow E_{\text{F}}$ ), which *lies lower in energy* than the purely molecular transition (see Figure 1). One consequence is that the charge-transfer terms in the SERS expansion lie lowest and, therefore (if the oscillator strengths are at all comparable), due to the smallness of the energy denominator, tend to contribute more to the SERS intensity than the corresponding molecular transition. These may provide the dominant contributions under some circumstances,

even to the totally symmetric normal modes. In the region of the spectrum where only the surface plasmon resonance is active (i.e., at an excitation wavelength far from the charge-transfer or molecular resonances), the charge-transfer states cannot be ignored because they appear in the sum over states expression and usually represent the leading terms in that sum. As shown above, when the excitation is in the region of a charge-transfer or molecular resonance, the influence of these transitions on the spectrum can come to dominate the appearance of the spectrum. This effect has been carefully delineated for the molecule *p*-aminothiophenol by Osawa and co-workers.<sup>30</sup>

A second important difference between SERS and normal Raman spectroscopy lies in the molecular orientation with respect to the surface. Note that normally, except for Raman spectra in crystals, the orientation of the molecule with respect to the polarization of the electric vector of exciting light is random, and in order to account for this, the expression for normal Raman spectroscopy is averaged over all orientations. For SERS, the molecule is usually considered to be adsorbed to the surface in a definite orientation. The surface plasmon resonance results in a very strong component of the electric field normal to the metal surface, with a somewhat smaller tangential component, at least for most molecule–metal configurations. In either case, the result is that the SERS spectrum of the molecule often looks quite different than that of the molecule alone. We cannot average over all molecular orientations with respect to the polarization of the exciting light. Although the molecular frequencies are usually not changed very much, the relative intensities are drastically altered in comparison to the normal Raman spectrum. Totally symmetric normal modes tend to dominate the spectrum far from charge-transfer or molecular transitions, while non-totally symmetric modes become considerably more prominent in the region of charge-transfer or molecular resonances. In this case the Herzberg–Teller-surface selection rules discussed in the previous section become important in interpreting the spectrum.

### Sorting Out the Various Contributions to SERS

We have shown above that there are three linked resonant contributions to the total SERS signal. At any chosen excitation wavelength, there might be quite different contributions from each resonance, but as the excitation wavelength is scanned, the relative degree of contribution from each resonance may vary considerably. This results in considerable variation of the appearance of the spectrum as a function of

excitation wavelength. In order to state with confidence the amount of contribution from each source, it is necessary to have a complete description of the location (in wavelength), the width, and the oscillator strength of each transition involved, as in Figures 4 and 5. Thus we need a good optical spectrum of the individual nanoparticles, the molecule, and if possible the molecule–metal system. This latter is often difficult to obtain, and an excitation profile of the SERS spectrum might suffice. In any case, it is impossible to determine the degree of contribution of each resonance by obtaining SERS spectra at only a single wavelength, unless there are other measures, such as an electrochemical voltage profile or a nanoparticle size-dependent profile.

We can obtain a quantitative measure of the relative charge-transfer or molecular resonance contribution to the SERS intensity by defining  $p_{CT}(k)$ , the degree of charge transfer for each mode as

$$p_{CT}(k) = \frac{I^k(CT) - I^k(SPR)}{I^k(CT) + I^0(SPR)} \quad (3)$$

where  $k$  is an index used to identify individual molecular lines in the Raman spectrum. We need the intensity of two reference lines obtained in a spectral region in which there is no charge-transfer contribution. One of these is  $I^k(SPR)$ , the intensity of the line ( $k$ ) in question taken where only the SPR contributes to the SERS intensity. This is ideally obtained in an electrochemical measurement at the same excitation wavelength (varying the applied potential) as the observed charge-transfer enhanced line. The other reference is a chosen totally symmetric line, also measured with only contributions from SPR. This is denoted  $I^0(SPR)$ .  $I^k(CT)$  is the measured intensity of the line ( $k$ ) in the region of the spectrum in which the charge-transfer resonance makes an additional contribution to the SERS intensity. It can be seen from eq 3 that when  $p_{CT}$  is zero, there are no charge-transfer contributions, while as  $p_{CT} \rightarrow 1$ , the charge-transfer contributions will tend to dominate the spectrum. For  $p_{CT} = 1/2$ , the charge-transfer and surface plasmon contributions are about equal. This expression has been successfully applied to the spectra of several molecules for which there is a sizable charge-transfer contribution to SERS, including *p*-aminothiophenol,<sup>18</sup> tetracyanoethylene, piperidine,<sup>38</sup> and crystal violet.<sup>31</sup> To determine the contribution from a molecular resonance, we may calculate  $p_{mol}(k)$  using the same formula as eq 3 with  $I^k(mol)$  substituted for  $I^k(CT)$ .

Note also that we now have a quantitative way of separating the A term contributions from the B or C term contributions. For totally symmetric modes,  $p_{CT}$  gives the A term



contribution plus any additional contribution from a nearby totally symmetric optical transition via either the B or C term. For non-totally symmetric modes,  $p_{CT}$  measures only the B or C term contributions.

## In Summary

In this Account, we have emphasized that a unified approach to SERS spectroscopy involves a model of the metal–molecule system in which three possible resonant enhancements are considered: excitations of the solid (SPR), excitations of the molecule (molecular resonance), and excitations involving metal–molecule coupling (CT resonances). All of these resonances are important in understanding the relative intensities of a SERS spectrum, and they are linked by symmetry considerations. A powerful means of elucidating this spectroscopy is the consideration of the Herzberg–Teller selection rules, which use the symmetry properties of the electronic dipole transition moments of the metal–molecule excitation normal to the surface and the molecular excitations. Modern electronic structure calculations of second-order molecular properties allow calculation of most of these properties with the exception of the Herzberg–Teller coupling parameter, which influences the intensity of the non-totally symmetric bands. Inclusion of this parameter in quantum mechanical calculations of spectral intensities, however, needs more development.

## BIOGRAPHICAL INFORMATION

**John R. Lombardi** was born in 1941 in Yonkers, New York. He attended Cornell University as an undergraduate working with A. C. Albrecht and received his Ph.D. from Harvard University in 1967 with Wm. Klemperer. He was assistant professor at the University of Illinois and is currently a Professor of Chemistry at The City College of New York. Other lines of interest include work with the Metropolitan Museum of Art on the Raman Spectroscopy of Dyes and Pigments used in paintings, textiles, and documents.

**Ronald L Birke** was born in 1939 in St. Louis, Missouri. He attended University of North Carolina (Chapel Hill) (B.S.), MIT (Ph.D.), and the Free University of Brussels (postdoctoral studies), where his mentors were Charles N. Reilley, David K. Roe, and Lucien Gierst, respectively. He was an instructor at Harvard University and an Associate Professor at the University of South Florida before coming to The City College of the City University of New York in 1974 where he is currently Professor of Chemistry. His interests are electrochemistry, bioinorganic chemistry of vitamin B<sub>12</sub> compounds, and Raman spectroscopy.

## REFERENCES

- Fleischmann, M. P.; Hendra, J.; McQuillan, A. J. Raman Spectra of Pyridine Adsorbed at a Silver Electrode. *Chem. Phys. Lett.* **1974**, *26*, 163–166.
- Jeanmaire, D. L. L.; Van Duyne, R. P. Surface Raman Spectroelectrochemistry. *J. Electroanal. Chem. Interfacial Electrochem.* **1977**, *84*, 1–20.
- Van Duyne, R. P. In *Chemical and Biochemical Applications of Lasers*; Moore C. B., Ed.; Academic Press: New York, 1979; Vol. 4, Chapter 5.
- Furtak, T. E. In *Advances in Laser Spectroscopy*; Garetz, B., Lombardi, J. R., Eds.; Wiley: Chichester, U.K., 1984; Vol. 2, p 175.
- Birke, R. L.; Lombardi, J. R. In *Advances in Laser Spectroscopy*; Garetz, B., Lombardi, J. R., Eds. Heyden: Philadelphia, PA, 1982; Vol. 1, p 143.
- Nie, S.; Emory, S. R. Probing Single Molecule and Single Nanoparticles by Surface-Enhanced Raman Scattering. *Science* **1997**, *275*, 1102–1106.
- Kneipp, K.; Wang, Y.; Kneipp, H.; Perelman, L.; Itzkan, I.; Dasari, R. R.; Feld, M. S. Single Molecule Detection Using Surface-Enhanced Raman Scattering. *Phys. Rev. Lett.* **1997**, *78*, 1667–1670.
- Xu, H.; Bjerneld, E.; Käll, M.; Börjesson, L. Spectroscopy of Single Hemoglobin Molecules by Surface Enhanced Raman Scattering. *Phys. Rev. Lett.* **1999**, *83*, 4357–4360.
- Schatz, G. C.; Young, M. A.; Van Duyne, R. P. In *Surface Enhanced Raman Scattering: Physics and Applications* Kneipp, K., Moskovits, M., Kneipp, H., Eds.; Topics in Applied Physics, Vol 103; Springer: Berlin, 2006, pp 19–64.
- Michaels, A. M.; Jiang, J.; Brus, L. E. Ag Nanocrystal Junctions as the Site for Surface-Enhanced Raman Scattering of Single Rhodamine 6G Molecules. *J. Phys. Chem. B* **2000**, *104*, 11965–11971.
- Bosnick, K. A.; Jiang, J.; Brus, L. E. Fluctuations and Local Symmetry in Single-Molecule Rhodamine 6G Raman Scattering on Silver Nanocrystal Aggregates. *J. Phys. Chem. B* **2002**, *106*, 8096–8099.
- Jiang, J.; Bosnick, K.; Maillard, M.; Brus, L. Single Molecule Raman Spectroscopy at the Junctions of Large Ag Nanocrystals. *J. Phys. Chem. B* **2003**, *107* (37), 9964–9972.
- Watanabe, T.; Yanagihara, N.; Honda, K.; Pettinger, B.; Moeri, L. Effects of Underpotentially Deposited Tl and Pb Submonolayers on the Surface-Enhanced Raman Scattering (SERS) from Pyridine at Ag Electrodes. *Chem. Phys. Lett.* **1983**, *96*, 649–655.
- Furtak, T. E.; Roy, D. Nature of the Active Site in Surface-Enhanced Raman Scattering. *Phys. Rev. Lett.* **1983**, *50*, 1301–1304.
- Hildebrandt, P.; Stockburger, M. Surface-Enhanced Resonance Raman Spectroscopy of Rhodamine 6G Adsorbed on Colloidal Silver. *J. Phys. Chem.* **1984**, *88*, 5935–5944.
- Zeman, E. J.; Carron, K. T.; Schatz, G. C.; Van Duyne, R. P. A surface Enhanced Resonance Raman Study of Cobalt Phthalocyanine on Rough Ag Films: Theory and Experiment. *J. Chem. Phys.* **1987**, *87*, 4189–4200.
- Lombardi, J. R.; Birke, R. L.; Lu, T.; Xu, J. Charge-Transfer Theory of Surface-Enhanced Raman Spectroscopy; Herzberg-Teller Contributions. *J. Chem. Phys.* **1986**, *84*, 4174–4180.
- Lombardi, J. R.; Birke, R. L. A Unified Approach to Surface-Enhanced Raman Scattering. *J. Phys. Chem. C* **2008**, *112*, 5605–5617.
- Campion, A. Kambhampati, Surface-Enhanced Raman Scattering. *Chem. Soc. Rev.* **1998**, *27*, 241–250.
- Kneipp, K.; Kneipp, H.; Itzkan, I.; Dasari, R. R.; Feld, M. S. Surface-Enhanced Raman Scattering and Biophysics. *J. Phys.: Condens. Matter* **2002**, *14*, R597–R624.
- Furtak, T. E.; Macomber, S. H. Voltage Induced Shifting of Charge-Transfer Excitations and Their Role in Surface-Enhanced Raman Scattering. *Chem. Phys. Lett.* **1983**, *95*, 328–332.
- Pockrand, I.; Otto, A. Surface-Enhanced and Disorder Induced Raman Scattering from Silver Films. *Solid State Commun.* **1981**, *37*, 109–112.
- Lombardi, J. R.; Birke, R. L.; Sanchez, L. A.; Bernard, I.; Sun, S. C. The Effect of Molecular Structure on Voltage-Induced Shifts of Charge-Transfer Excitation in Surface Enhanced Raman Scattering. *Chem. Phys. Lett.* **1984**, *104*, 240–247.
- Burstein, E.; Chen, Y. J.; Lundquist, S.; Tosatti, E. Giant Raman Scattering by Adsorbed Molecules on Metal Surfaces. *Solid State Commun.* **1979**, *29*, 567–570.
- Persson, B. N. J. On the Theory of Surface-Enhanced Raman Scattering. *Chem. Phys. Lett.* **1981**, *82*, 561–565.
- Gersten, J. I.; Birke, R. L.; Lombardi, J. R. Theory of Enhanced Light Scattering from Molecules Adsorbed at the Metal-Solution Interface. *Phys. Rev. Lett.* **1979**, *43*, 147–150.
- Otto, A.; Mrozek, I.; Grabhorn, H.; Akemann, W. Surface Enhanced Raman Scattering. *J. Phys.:Condens. Matter* **1992**, *4*, 1143–1153.
- Albrecht, A. C. On the Theory of Raman Intensities. *J. Chem. Phys.* **1961**, *34*, 1476–1484.
- For simplicity, we have chosen a term from the C (metal-to-molecule charge transfer) expression. In order to obtain corresponding expressions for the B (molecule-to-metal) expression, it suffices to interchange I and K.



- 30 Osawa, M.; Matsuda, N.; Yoshii, K.; Uchida, I. Charge-Transfer Resonance Raman Process in Surface-Enhanced Raman Scattering from *p*-Aminothiophenol Adsorbed on Silver: Herzberg–Teller Contribution. *J. Phys. Chem.* **1994**, *98*, 12702–12707.
- 31 Cañamares, M.; Chenal, C.; Birke, R. L.; Lombardi, J. R. DFT, SERS, and Single Molecule-SERS of Crystal Violet. *J. Phys. Chem. C* **2008**, *112*, 20295–20300.
- 32 Watanabe, T.; Pettinger, B. Surface-Enhanced Raman Scattering from Crystal Violet Adsorbed on a Silver Electrode. *Chem. Phys. Lett.* **1982**, *89*, 501–507.
- 33 We have chosen here a particular sample of Ag nanoparticles produced photochemically in our laboratory for the SPR absorption. By varying the growth conditions, samples with quite different SPR profiles can be obtained. See, for example: Zheng, X. L.; Xu, W. Q.; Corredor, C.; Xu, S. P.; An, J.; Zhao, B.; Lombardi, J. R. *J. Phys. Chem. C* **2007**, *111*, 14962–14967.
- 34 Uwada, T.; Toyota, R.; Masuhara, H.; Asahi, T. Single Particle Spectroscopic Investigation of the Interaction between Exciton Transition of Cyanine Dye J-Aggregates and Localized Surface Plasmon Polarization of Gold Nanoparticles. *J. Phys. Chem. C* **2007**, *111*, 1549–1552.
- 35 Kelley, A. M. A Molecular Spectroscopic Description of Optical Spectra of J-Aggregated Dyes on Gold Nanoparticles. *Nano Lett.* **2007**, *7*, 3235–3240.
- 36 Kelley, A. M. A Molecular Spectroscopic View of Surface Plasmon Enhanced Resonance Raman Scattering. *J. Chem. Phys.* **2008**, *128*, 224702–224708.
- 37 Conversely, the orientation of the molecule with respect to the surface can be inferred by observation of the relative intensities of the SERS spectrum.
- 38 Chenal, C.; Birke, R. L.; Lombardi, J. R. Determination of the Degree of Charge-Transfer Contributions to Surface Enhanced Raman Spectroscopy. *ChemPhysChem* **2008**, *9*, 1617–1623.
- 39 Aikens, C. M.; Li, S.; Schatz, G. C. From Discrete Electronic States to Plasmons: TDDFT Optical Absorption Properties of  $Ag_n$  ( $n = 10, 20, 35, 56, 84, 120$ ) Tetrahedral Clusters. *J. Phys. Chem. C* **2008**, *112*, 11272–11279.
- 40 Innes, K. K.; Byrne, J. P.; Ross, I. G. Electronic States of Azabenzenes: A Critical Review. *J. Mol. Spectrosc.* **1967**, *22*, 125–147.
- 41 Yamada, H.; Nagata, H.; Toba, K.; Nakao, Y. Charge-Transfer Band and SERS Mechanism for the Pyridine-Ag System. *Surf. Sci.* **1987**, *182*, 269–286.
- 42 Seki, H. SERS Excitation Profile of Pyridine and CO on Silver in UHV. *J. Electroanal. Chem.* **1983**, *150*, 425–436.
- 43 Lovell, S.; Marquardt, B. J.; Kahr, B. Crystal Violet's Shoulder. *J. Chem. Soc., Perkin Trans 2* **1999**, 2241–2247.
- 44 Chou, Y. C.; Liang, N. T.; Tse, W. S. Enhancement of Resonance Raman Scattering from Crystal Violet Deposited on Island Silver Films. *J. Raman Spectrosc.* **1986**, *17*, 481–489.
- 45 Jiang, J. D.; Burstein, E.; Kobayashi, H. Resonant Raman Scattering by Crystal Violet Molecules Adsorbed on a Smooth Gold Surface: Evidence for a Charge-Transfer Excitation. *Phys. Rev. Lett.* **1986**, *57*, 1793–1796.